View Online / Journal Homepage / Table of Contents for this issue
Dynamic Article Links

Lab on a Chip

Cite this: *Lab Chip*, 2012, **12**, 558

www.rsc.org/loc

COMMUNICATION

Microfluidic capture and release of bacteria in a conical nanopore array†

Peng Guo,‡[ab] Eric W. Hall,[a] Romana Schirhagl,[a] Hitomi Mukaibo,[b] Charles R. Martin[b] and Richard N. Zare*[a]

Received 10th November 2011, Accepted 30th November 2011
DOI: 10.1039/c2lc21092d

Published on 30 November 2011 on http://pubs.rsc.org | doi:10.1039/C2LC21092D
Downloaded by Stanford University on 19 February 2012

We present a simple and inexpensive method for the capture and release of bacteria contained in an array of conical nanopores on a membrane inside a microfluidic device. As an example, we demonstrate that cyanobacteria can be captured, one bacterium per pore, in a defined orientation with over 500 bacteria per membrane with viabilities as high as 100%. The device can also specifically capture cyanobacteria from a mixed suspension of cyanobacteria and chlamydomonas with a selectivity as high as 90%.

Quantitative single-cell analysis is essential for drug screening,[1] cellular metabolism,[2] population evolution,[3] and phenotypic differentiation screening.[4] In this paper, we present a simple and inexpensive technique for capture and release of bacteria, contained one per pore, in a conical nanoporous membrane (CNM) integrated into a microfluidic chip. This study, to our knowledge, is the first investigation into the possibility of using conical nanopores for capture and release of cells.

We chemically etched a track-damaged polymeric membrane to generate arrays of conical nanopores on the membrane. The diameters of the conical nanopores were precisely controlled to capture only one bacterium per pore. Pressure-driven flow was applied to move a suspension of bacteria through the membrane that had been incorporated into a microfluidic device, trapping individual bacteria within an array of conical nanopores. Trapped bacteria were released by reversing the direction of the pressure-driven flow. Surface modification of either the CNM or the microfluidic channel was not required during the experimental process. To demonstrate a biological application of this method for bacteria manipulation, we selected cyanobacteria for capture-and-release studies. Cyanobacteria contain fluorescent proteins, such as phycobilin, which allow them to be tracked *via* laser fluorescence microscopy.[5] Further, we have demonstrated selectivity of capture by injecting a mixture of cyanobacteria and *Chlamydomonas reinhardtii*. Full experimental details may be found in the Supplementary Information document.

We used the asymmetric track-etch method reported previously by Martin and co-workers,[6,7] where conical nanopores with well-controlled dimensions are etched into a polyethylene terephthalate (PET) membrane (Fig. 1a). In our experiment, diameters of the base (D_{base}) and tip (D_{tip}) openings were controlled to be 1.30 ± 0.05 μm and 270 ± 139 nm, respectively. Compared with the diameter of cyanobacteria (D_{cyano} = 800 nm), $D_{tip} < D_{cyano} < D_{base} < 2 \times D_{cyano}$, these dimensions allow only one bacterium to be trapped within one conical nanopore at a time. Base and tip diameters were determined *via* scanning electron microscopy (Fig. 1b). Internal morphology of the nanopores was characterized by depositing gold *via* electroless plating and removing the membrane, as described in detail previously[8–10] and in the accompanying Supplementary Information document. These gold structures, shown in Fig. 1c, confirmed the formation of conical nanopores throughout the PET membrane.

A three-layer microfluidic design[11] was chosen to generate the conical nanoporous membrane-based bacteria capture-and-release chip (CNM-C&R chip), consisting of a top layer, a CNM, and

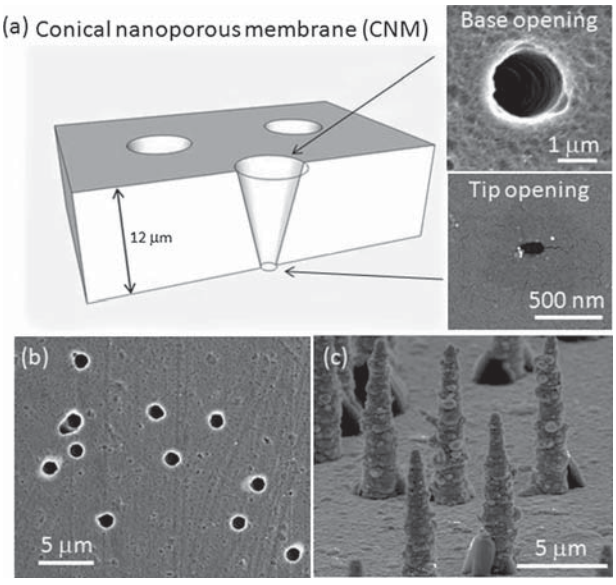

Fig. 1 Characterization of the conical nanoporous membrane. (a) Cross-section scheme of one conical nanopore in a PET membrane. Two images on right are SEM images of base and tip openings of one conical nanopore. (b) SEM image showing randomly patterned conical nanopores. (c) SEM image showing gold replicas representing the internal morphology of conical nanopores.

[a]*Department of Chemistry, Stanford University, Stanford, California, 94305-5080, USA. E-mail: zare@stanford.edu; Fax: +1 650 725-0259; Tel: +1 650 723-3062*
[b]*Department of Chemistry, University of Florida, Gainesville, Florida, 32611-7200, USA*
† Electronic supplementary information (ESI) available. See DOI: 10.1039/c2lc21092d
‡ Present address: School of Engineering and Applied Sciences, Harvard University, Cambridge, Massachusetts, 02138, USA.

This journal is © The Royal Society of Chemistry 2012

Downloaded by Stanford University on 19 February 2012
Published on 30 November 2011 on http://pubs.rsc.org | doi:10.1039/C2LC21092D

a bottom layer (as shown in Fig. 2a). Both top and bottom layers consist of polydimethylsiloxane (PDMS) with a microfluidic chamber and channels fabricated *via* soft lithography. As shown in Fig. 2a, the top layer contains a cell capture chamber, cylindrical in shape, 1000 μm in diameter and 20 μm in height. Three microfluidic channels are connected to the capture chamber in the top layer: one inlet channel for injection of the bacterium suspension and two side channels for use in flushing. All three channels have a height of 20 μm and a width of 100 μm. The channel structure on the bottom layer does not have side channels. The CNM is sandwiched between the top and bottom layers, fixed with a PDMS mortar,[12] with the base openings of the conical nanopores facing toward the capture chamber in the top layer (Fig. 2b). This allows bacteria in the inlet channel to enter the conical nanopores *via* their base openings. Fabrication details may be found in the accompanying Supplementary Information.

The mechanisms of capture and release are elaborated in Fig. 3a. For bacteria capture, a flow was created with negative pressure (2000 Pa) for five minutes. The flow direction originated from the inlet channel, through the CNM (from the base toward the tip), and finally into the outlet channel. Cyanobacteria in the suspension were transported by the flow and moved into the base opening of one conical nanopore each. After bacteria capture, phosphate buffered saline (PBS) at pH 7.4 was injected through the side channels across the capture chamber to wash the surface of the conical nanoporous membrane and remove nonspecific bacteria adsorption. PBS flushing was performed three times.

For bacteria release, side channels in the top layer were first closed simply by inserting metal rods into their inlets. PBS was injected in the reverse direction of that used for capture, for five minutes. This was repeated three times. Cyanobacteria trapped within conical nanopores were released with PBS into the inlet channel in the top layer. Any remaining nonspecific bacteria adsorption was removed by flushing PBS across the membrane *via* the side channels.

All processes were monitored using a CCD camera (Mintron MTV-63KR11N) and an inverted microscope (Nikon Eclipse TE2000-U). A diode laser (Crysta Laser, max. output power: 495 mW, 633 nm) was expanded *via* an optical set-up to cover an area of approximately 400 μm × 400 μm within the separation device, which can be regarded as the detection area, to visualize cyanobacteria.

Cell viability of cyanobacteria after capture and release was determined by a L7012 LIVE/DEAD® BacLight Bacterial Viability Kit according to the manufacturer's specifications. Capture and release was performed as described above. Captured cyanobacteria were held for 1, 2, and 3 h then released and directly collected for live/dead staining. Suspensions held in the chip, but not subjected to capture, were used as controls.

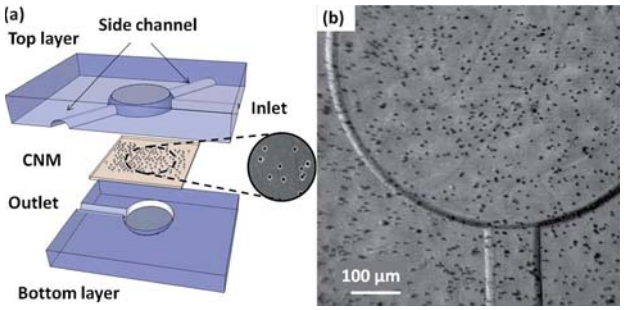

Fig. 2 Fabrication of CNM-C&R chip. (a) Scheme of three-layer design of CNM-C&R chip. The top layer contains one chamber and three channels (one inlet and two side channels). The bottom layer contains one chamber and one outlet channel. The CNM is sandwiched between them. Base openings in CNM face the chamber in the top layer. (b) Bright-field microscope image showing partially assembled CNM-C&R chip.

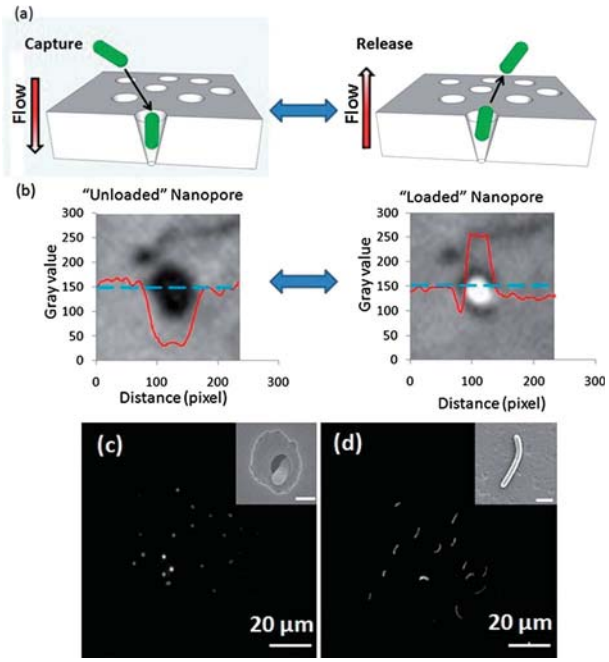

Fig. 3 Mechanism of bacteria capture and release. (a) Scheme of single-cell capture and release in CNM. (b) Fluorescence microscope images of one conical nanopore unloaded (left) and loaded (right) with one cyanobacterium, including brightness profiles (red curves) along a row of pixels (blue lines) through the images. Fluorescence microscope images of trapped cyanobacteria in CNM (c) and free cyanobacteria on flat PET membrane as control (d). Insets are SEM images of trapped (c) and free (d) cyanobacteria.

To investigate the selectivity of capture, we made mixed suspensions of cyanobacteria (Cyano) and *Chlamydomonas reinhardtii* (Chlamy) at different varying ratios (1 : 1, 3 : 7, 1 : 9 Cyano/Chlamy) and tried to selectively capture cyanobacteria from them using the CNM-C&R chip. Chlamydomonas cells were selected because they are common green algae that widely coexist with cyanobacteria within many natural environments.[13] The competition between cyanobacteria and chlamydomonas for nutrients and light induces cyanobacteria to release antialgal toxins.[13] Additionally, chlamydomonas has a spherical shape with a diameter of about 6 μm, while *Synehococcus* cyanobacteria have a rod-like morphology that is 800 nm in its smaller diameter and 4 μm in its larger diameter. All Cyano/Chlamy mixed suspensions used in this experiment contained a total cell concentration of 10^7 cells mL^{-1}. Capture and release was performed according to the aforementioned protocol. The number of trapped cells in the CNM was determined by fluorescence microscopy.

Capture of bacteria, one per pore, in the CNM was achieved, as demonstrated in Fig. 3. We used ImageJ software to plot the brightness profiles of images of a conical nanopore, one loaded with a cyanobacterium and one without, and found that the brightness of a loaded nanopore was significantly higher than that of an unloaded one (Fig. 3b). This was due to the strong fluorescence intensity from

Downloaded by Stanford University on 19 February 2012
Published on 30 November 2011 on http://pubs.rsc.org | doi:10.1039/C2LC21092D

the trapped cyanobacterium. It is also important to mention that all captured cyanobacteria were held in the same orientation, which is vertical with respect to the CNM. Fluorescence images of the cells trapped within the pores of the membrane (Fig. 3c) are uniformly circular, while images of free cells on a flat, nonporous PET surface (Fig. 3d) range from circular to ovular. This is due to the rod-like shape of cyanobacteria, which appear as circles when viewed vertically and as rods when viewed horizontally. These observations were further confirmed by SEM (insets of Fig. 3c and 3d). The CNM could also be specifically prepared to capture a wide range of sub-micron analytes by tuning its pore size and shape. Martin's lab has successfully demonstrated reproducible preparation of the conical nanopore with a tip diameter of 10 nm,[6,7] and achieved a minimum tip diameter of 1 nm with gold plating.[14] In our study, we also captured *E. coli* bacteria and virus-sized polystyrene nanoparticles (100 nm in diameter), as shown in the Fig. S1.

We also demonstrated that the capture capacity of the CNM-C&R chip was controllable with different pore densities. Two CNMs with different pore densities (10^6/cm^2 and 10^5/cm^2) were used to fabricate the CNM-C&R chip. The resulting chips were tested for cyanobacteria over five capture-and-release cycles. Under the same experimental conditions, capture capacities of the 10^6/cm^2 and 10^5/cm^2 CNMs were 560 ± 83 cells and 220 ± 34 cells, respectively; and capture efficiencies were 7 ± 1% and 28 ± 4%, respectively (as shown in Fig. 4a and 4c). Low capture efficiencies probably result from the geometrical constraints on capture. Due to the rod-like shape of cyanobacteria and the conical shape of our nanopores, there are two requirements for cyanobacteria capture: (1) bacteria need to be vertical to the CNM; and (2) one end of the rod-like bacterium needs to face approximately into the base opening of a nanopore. Only when these two requirements are satisfied, can bacteria enter the nanopore and be captured. Some bacteria that could not enter the nanopores were nonspecifically adsorbed onto the CNM surface. This may create steric hindrances for other cells, causing a decrease in capture efficiency. This is evidenced by the fact that 10^6/cm^2 CNMs were observed to possess lower capture efficiencies than 10^5/cm^2 CNMs. For a certain capture time (5 min) and pressure (2000 Pa), the flow volume of cyanobacteria suspension through a 10^6/cm^2 CNM was 10 times larger than that of 10^5/cm^2 conical nanoporous membrane due to its higher pore density. This causes about 10 times more nonspecifically adsorbed bacteria to be accumulated on the CNM surface, and creates a much greater steric hindrance. As a result, the capture efficiency of 10^6/cm^2 (7%) is lower than that of 10^5/cm^2 (28%).

After releasing cyanobacteria and flushing three times with phosphate-buffered saline (PBS), 91% and 77% captured cyanobacteria were released from the 10^6/cm^2 and 10^5/cm^2 CNM chips, respectively. The release efficiency (Eff_R) was calculated by the following formula

$$Eff_R = (1 - Bac_{After}/Bac_{Before}) \times 100\%$$

where Bac_{Before} and Bac_{After} are the numbers of bacteria trapped on the membrane before and after a release and wash steps.

For 10^6/cm^2 and 10^5/cm^2 CNMs, average bacteria numbers after release are almost the same (52 and 50, respectively), and average bacteria numbers before release are 560 and 220, respectively. Therefore, the release efficiency is 91% for 10^6/cm^2 CNM and 77% for 10^5/cm^2 CNM. Capture-and-release cycles in 10^6/cm^2 and 10^5/cm^2 CNM-C&R chips were repeated five times (shown in Fig. 4b and 4d) to confirm that the CNM-C&R chip is stable and reproducible over multiple uses.

Results of the viability study are shown in Fig. 5. Viability of cyanobacteria subjected to a 1 h hold time on the CNM-C&R chip were 100% alive, which is the same as that of an uncaptured control. After 2 h and 3 h hold times, capture-and-release cyanobacteria viabilities decreased to 89 ± 4% and 69 ± 10%, respectively. These numbers were slighter lower than viabilities of the controls: 92 ± 7% and 82 ± 10%. This means that the act of capture within nanopores has a weak negative effect on bacteria viability. But after a 3 h hold time viability of capture-and-release cells was still close to 70%. This has also been seen in other bacteria research.[15,16] Brinker and co-workers[15] reported that confinement of individual *Staphylococcus aureus* bacteria could induce quorum sensing (cell-cell communication) and maintain bacteria viability. Ismagilov and co-workers[16]

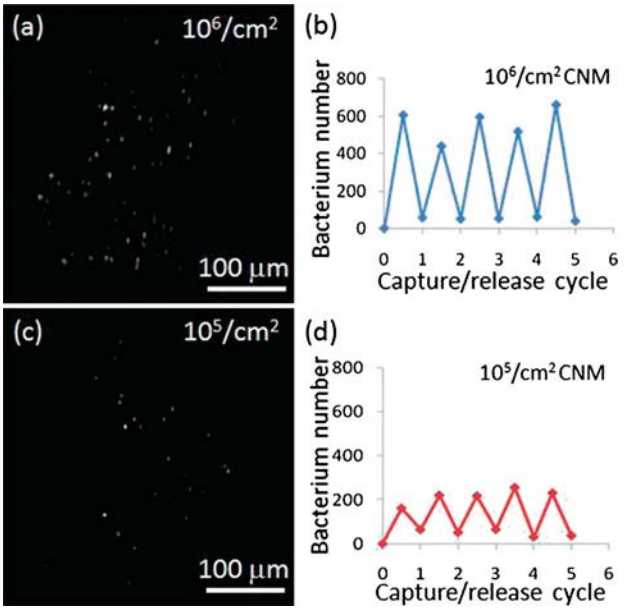

Fig. 4 Characterization of cyanobacteria capture and release cycles. (a and c) Fluorescence microscope images of single bacteria captured in an array of nanopores within CNM-C&R chips with different pore densities: 10^6/cm^2 (a) and 10^5/cm^2 (c). (b and d) Number of cyanobacteria trapped in CNM during capture-and-release cycles.

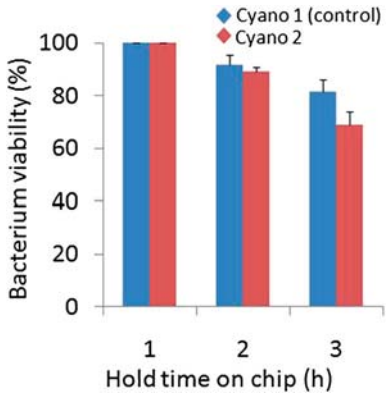

Fig. 5 Bacteria viability after capture-and-release cycles with different hold times: 1, 2 and 3 h. Untreated cyanobacteria were used as controls.

This journal is © The Royal Society of Chemistry 2012

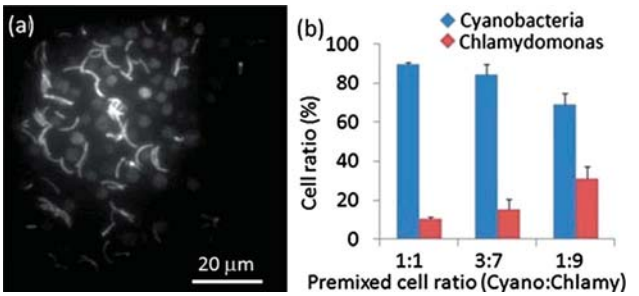

Fig. 6 Selectivity of single-bacteria capture within conical nanopores. (a) Fluorescence microscope image of Cyano/Chlamy mixed suspensions at a cell concentration ratio of 1 : 1. (b) Cell ratio of cyanobacteria and chlamydomonas after selective capture. Three Cyano/Chlamy mixed suspensions with different cell concentration ratios, 1 : 1, 3 : 7, and 1 : 9, are tested. Values shown are means ± one standard deviation from triplicate experiments.

found that microfluidic confinement of individual *Pseudomonas aeruginosa* bacteria can initiate quorum sensing and achieve quorum sensing-dependent growth. We found a cell viability decrease in control cells over 3 h in our study. This viability decrease is probably caused by the stress experienced by cyanobacteria in PBS solution. Both capture-and-release and control cyanobacteria were suspended in PBS in our experiment, not the carbon-dioxide-infused BG-11 culture media in which these bacteria are typically grown.

Selective capture between cyanobacteria (Cyano) and *Chlamydomonas reinhardtii* (Chlamy) is based on the size difference between Cyano and Chlamy. Cyano has a rod-like shape with a diameter of 800 nm and a length of 4–6 μm; Chlamy has a spherical shape with a diameter of 6 μm. In our experiment, each conical nanopore has an identical base diameter (1.3 μm) and tip diameter (270 nm). Thus, Cyano could enter and be captured by the conical nanopore, whereas Chlamy could not. During the rinsing step, most Chlamy adsorbed onto the CNM surface could be removed, leaving only captured Cyano in the CNM-C&R chip. The results of the selective capture study are shown in Fig. 6a and 6b. The capture ratio of Cyano over all captured cells on the CNM-C&R chip is 90 ± 2%, 85 ± 10%, and 69 ± 12% for 1 : 1, 3 : 7, and 1 : 9 Cyano/Chlamy mixed suspensions. The Cyano capture ratios decrease in 3 : 7 and 1 : 9 Cyano/Chlamy mixed suspensions, because there are less Cyano captured in the CNM and more Chlamy nonspecifically adsorbed onto the CNM surface. But, even with a Chlamy-dominant suspension with a very low abundance of cyanobacteria (Cyano:Chlamy, 1 : 9), the CNM-C&R chip could still produce a capture population that was more than 50% Cyano.

In summary, we have developed a simple and straightforward method to capture and release bacteria in an array of conical nanopores, one bacterium per pore, within a membrane integrated into a microfluidic platform. Additionally, cells were aligned differently than in other methods, which could be advantageous for some studies on cell-directed behaviors, such as bacteria-directed division in filament formation. A future extension of our methodology is production of an ordered conical nanopore pattern which allows quantitative mapping and tracking of multiple individual targets during high-throughput single-cell analysis. The remarkable ability of the track-etch method to generate arrays of asymmetric nanopores with diameters down to a few nanometres enables us to extend this technique to various kinds of nanoscale biological analytes such as bacteria, viruses, proteins, DNA and small signaling molecules. Compared with current single-cell trapping techniques, the track-etched conical nanoporous membrane is inexpensive, less demanding to use, and easy to scale up. This technology appears to be well suited for use in future lab-on-a-chip experiments.

We are grateful to Devaki Bhaya and Michelle Davison, Department of Plant Biology, Carnegie Institution for Science, for supplying cells to us. We thank the National Science Foundation (grant award MCB-0749638-002) for supporting this project.

Notes and references

1 P. O. Krutzik, J. M. Crane, M. R. Clutter and G. P. Nolan, *Nat. Chem. Biol.*, 2007, **4**, 132–142.
2 S. N. Krylov, Z. Zhang, N. W. Chan, E. Arriaga, M. M. Palcic and N. J. Dovichi, *Cytometry*, 1999, **37**, 14–20.
3 L. Keller and M. G. Surette, *Nat. Rev. Microbiol.*, 2006, **4**, 249–258.
4 W. K. Smits, O. P. Kuipers and J.-W. Veening, *Nat. Rev. Microbiol.*, 2006, **4**, 259–271.
5 S. Joshua and C. W. Mullineaux, *Plant Physiol.*, 2004, **135**, 2112–2119.
6 J. E. Wharton, P. Jin, L. T. Sexton, L. P. Horne, S. A. Sherrill, W. K. Mino and C. R. Martin, *Small*, 2007, **3**, 1424–1430.
7 H. Mukaibo, L. P. Horne, D. Park and C. R. Martin, *Small*, 2009, **5**, 2474–2479.
8 S. Yu, N. Li, J. Wharton and C. R. Martin, *Nano Lett.*, 2003, **3**, 815–818.
9 P. Scopece, L. A. Baker, P. Ugo and C. R. Martin, *Nanotechnology*, 2006, **17**, 3951–3956.
10 V. P. Menon and C. R. Martin, *Anal. Chem.*, 1995, **67**, 1920–1928.
11 H. Wei, B.-han Chueh, H. Wu, E. W. Hall, C.-wing Li, R. Schirhagl, J.-M. Lin and R. N. Zare, *Lab Chip*, 2011, **11**, 238.
12 B.-han Chueh, D. Huh, C. R. Kyrtsos, T. Houssin, N. Futai and S. Takayama, *Anal. Chem.*, 2007, **79**, 3504–3508.
13 R.-B. Volk and F. H. Furkert, *Microbiol. Res.*, 2006, **161**, 180–186.
14 C. R. Martin, M. Nishizawa, K. Jirage and M. Kang, *J. Phys. Chem. B*, 2001, **105**, 1925–1934.
15 E. C. Carnes, D. M. Lopez, N. P. Donegan, A. Cheung, H. Gresham, G. S. Timmins and C. J. Brinker, *Nat. Chem. Biol.*, 2009, **6**, 41–45.
16 J. Q. Boedicker, M. E. Vincent and R. F. Ismagilov, *Angew. Chem.*, 2009, **121**, 6022–6025.

Downloaded by Stanford University on 19 February 2012
Published on 30 November 2011 on http://pubs.rsc.org | doi:10.1039/C2LC21092D